



A novel circadian daylight metric for building design and evaluation



Kyle Konis

University of Southern California, United States

ARTICLE INFO

Article history:

Received 9 June 2016

Received in revised form

8 November 2016

Accepted 12 November 2016

Available online 14 November 2016

Keywords:

Daylighting

Circadian system

Climate based daylight modeling

Daylighting metrics

Health

ABSTRACT

This paper extends the applicability of emerging frameworks for evaluating the non-visual effects of light through the development of a novel area-based daylighting metric addressing goals of human circadian stimulus and entrainment in buildings. Procedures using annual, climate-based daylight modeling of eye-level light exposures are developed to analyze and map indoor environments in regard to spatial and seasonal changes in the availability of a circadian-effective daylight stimulus. Because the biological effects of light exposure are not instantaneous, a novel approach is developed to assess the duration of an effective stimulus on a daily basis, as well as the frequency an effective stimulus is present over the course of a year. Results can be used to identify and visually examine building zones where long-term occupancy may lead to disruption of the circadian system in the absence of supplemental electrical lighting capable of effective circadian stimulus. The metric and visualization techniques are implemented in a parametric, simulation-based workflow utilizing publicly available software tools. The workflow can be used to assess and differentiate the performance of various daylighting strategies during the design phases of a project, or to examine existing spaces. The applicability of the workflow is demonstrated using two example models: a portable school classroom, and a generic open-plan commercial office floor plate.

© 2016 Elsevier Ltd. All rights reserved.

1. Introduction

Standards and practices for lighting design were developed to serve human visual needs prior to scientific understanding of the important role light plays in maintaining healthy human biological functions. The discovery of a third class of photoreceptors in the human retina [1–4], referred to as Intrinsically Photoreceptive Retinal Ganglion Cells (ipRGCs), has led to a growing interest in the non-visual effects of light on human health and well-being. In contrast to rod and cone photoreceptors, which serve as inputs for low-light and color vision, the ipRGCs serve no visual (image-forming) function. Instead, ipRGCs play a critical role in synchronizing human *circadian rhythms* to the 24-h light/dark cycle of the local environment. Notably, the action spectrum of light for the circadian system is shifted towards shorter wavelength (~490 nm) “blue” light relative to the visual system, which is maximally sensitive to (~555 nm) “green” light [5,6]. As a result, humans are not well equipped to self-report the presence or intensity of circadian-effective light based on visual perception.

Inside buildings, where adults spend 87% of their lives on

average [7], lighting is often provided by electrical sources that are adequate for performance of visual tasks (i.e. stimulation of the visual system), but can lack the appropriate spectral composition and intensity required to stimulate the circadian system. All zones within a building that do not regularly achieve the lighting conditions necessary for effective circadian stimulus can be labeled as *biologically dark*, and considered as zones where sustained occupancy over extended time periods (e.g. regular workday schedules) may present a risk for disruption of the circadian system in the absence of supplemental electrical lighting capable of effective circadian stimulus.

As evidence of the health impacts of light exposure grows, it is import for designers to have metrics and guidance to evaluate project performance in regard to the non-visual effects of light alongside more commonly used lighting metrics related to visual task performance (e.g. horizontal workplane illuminance and illuminance uniformity), visual discomfort (e.g. probability of glare), lighting energy savings (e.g. electrical lighting energy reduction from photocontrols), and Indoor Environmental Quality (IEQ) (e.g. compliance with the U.S. Green Building Council’s LEED Daylighting Environmental Quality (EQ) credit [8]).

There are currently no minimum requirements for daylight access in buildings to support circadian entrainment. However, the

E-mail address: kskonis@gmail.com.

International WELL Building Institute has recently developed a building certification system with the stated objective of, “measuring, certifying and monitoring the performance of building features that impact health and well-being” [9]. One of the pre-conditions for certification, (entitled “Circadian Lighting Design”), is the provision of sufficient melanopic light intensity for work areas. The term “melanopic” refers to a new photometric measure of light intensity weighed by the sensitivity of the melanopsin-containing ipRGCs, and is discussed further in Section 2.1. While the precondition does not require the use of daylight to meet the requirement, the contribution of daylight can be included in simulation-based predictions (the specific compliance criteria and their current ambiguities are discussed in greater detail in the following sections). Despite the fact that compliance can be achieved exclusively through the use of electrical lighting, it is anticipated that designers will seek to meet such requirements to the extent possible through the use of daylight, and supplement insufficiently-daylit zones with appropriate electrical lighting.

The emergence of requirements for circadian lighting design signals a growing interest in the challenge of translating scientific knowledge into actionable information that can be applied to improve the well-being of building occupants. It should be emphasized that the development of a circadian daylight metric relies on a combination of available scientific information and expert judgments related to the timing, intensity, duration, wavelength and past history of light exposures. A rationale for how each of these factors is addressed is included in this paper along with discussion of additional factors that are not directly related to building design, such as age and work schedule requirements. The reader should expect the judgments made in this paper to be revisited as scientific understanding of the human non-visual response to light evolves. Nevertheless, it is important for designers to have access to design support tools and performance criteria developed on available knowledge to specifically address non-visual effects of light during design. Such tools can help designers to better assess, understand and improve the circadian effectiveness of various daylighting strategies.

This paper extends the applicability of emerging frameworks for evaluating the non-visual effects of light through the development of a novel area-based daylighting metric addressing goals of human circadian stimulus and entrainment in buildings. Procedures using annual, climate-based daylight modeling of eye-level light exposures are developed to analyze and map a space in terms of the frequency of a circadian-effective daylight stimulus. Because the biological effects of light exposure are not instantaneous, a novel approach is developed to assess the duration of an effective stimulus on a daily basis, as well as the frequency an effective stimulus is present over the course of a year. Results can be used to identify, quantify and visually examine building zones where long-term occupancy may lead to disruption of the circadian system in the absence of supplemental electrical lighting capable of effective circadian stimulus. The metric and visualization techniques are implemented in a parametric, simulation-based workflow utilizing publicly available software tools. The workflow can be used to assess and differentiate the performance of various daylighting strategies during the design phases of a project, or to examine existing spaces. The workflow files are available for download here [10]. The applicability of the workflow is demonstrated using two example models: a portable school classroom, and a generic open-plan commercial office floor plate.

2. Previous work

There are a number of parameters known to control the circadian system's response to light that are directly impacted by

building design. These include the timing, intensity, duration, wavelength and past history of light exposures [11]. The following sections describe the rationale and assumptions made in regard to each of these parameters to develop a procedure to analyze and map a space in terms of the frequency of a circadian-effective daylight stimulus.

2.1. Spectrum and intensity of light exposure

To study the potential circadian effects of various light sources it is first necessary to quantify light exposure in biologically meaningful units. Fig. 1 shows the spectral efficiency function of the melanopsin-containing ipRGCs (black curve) developed by Enezi et al. and Lucas et al. [12,13], referred to as the melanopic spectral efficiency function (annotated here as C-lambda). The melanopic spectral efficiency function can be used to calculate melanopic illuminance (reported in units of Equivalent Melanopic Lux (EML)) for various light source Spectral Power Distributions (SPD) [14]. Fig. 1 also shows the spectral efficacy function of the visual (photopic) system (V-lambda) along with the SPDs of three Commission Internationale de l'Eclairage [15 CIE] daylight illuminants, (D55) sunlight, (D65) overcast sky, and (D75) north sky daylight. Fig. 1 shows that the maximum efficacy of the circadian system (C-lambda) is more closely aligned with the maximum power of the three daylight SPDs compared with the photopic function (V-lambda). In contrast, Fig. 2 compares the spectral response of the visual system (V-lambda) and the circadian system (C-lambda) to the spectral power distribution of a “standard” fluorescent lamp, (CIE illuminant F11), which represents a narrow tri-band fluorescent of 4000° Kelvin color temperature. Fig. 2 shows that the peak power of two of the three most prominent wavelength bands fall largely outside sensitivity of the circadian system (C-lambda). The introduction of EML as a unit enables designers to differentiate the relative “circadian efficacy” of various light sources (such as daylight vs. fluorescent) that may produce the same visual effect.

Several researchers have proposed models of the spectral sensitivity of the circadian system that can be used to relate the SPD from various light sources to objective and subjective stimulus effects. The model developed by Rea et al. [16] is based on published studies of nocturnal melatonin suppression using lights of various SPDs. The model relates a given SPD to a Circadian Stimulus (CS) effect from 0% (no effect) to 70% (maximum suppression level achievable after 1-h) characterizing the relative effectiveness of the source as a stimulus. The model can be applied to convert various light sources to units of Circadian Lux (CL_A) for relative comparison using a publicly available circadian stimulus calculator [17]. The model developed by Andersen et al. [18] is based on both nighttime [19] and daytime [20] studies and “sets a tentative lower and upper bound for the likelihood that a given light exposure will have an effect on alertness,” with a liner ramp-function applied to interpret intermediate values. The upper and lower bounds of the model can be converted into the standard photometric unit of illuminance (lux) using the approach described in Pechacek et al. [21] for any SPD of interest by applying a conversion factor. For example, for D65, the lower bound is 190 lux, and the upper bound is 870 lux. Finally, Amundadottir et al. [22] have developed a framework to describe the circadian effectiveness of light that can be explored using an online calculation and visualization tool [23]. The framework incorporates dose-response models of melatonin suppression, melatonin phase shift, and perceived alerting effect, enabling users to predict and compare the biological effect for various light source SPDs. The framework incorporates a lens transmittance model [24] and requires the user to specify the age of the observer to account for the relative loss in retinal exposure due to age. In specifying any threshold level, the age of the occupants is an

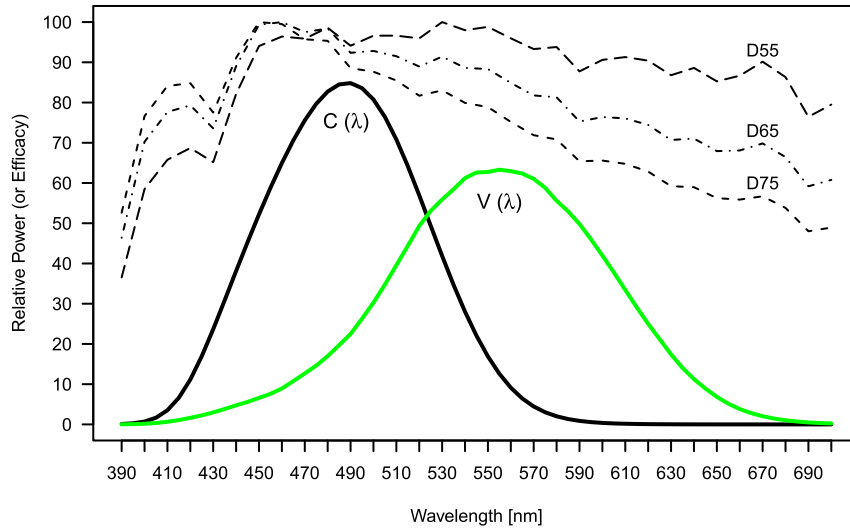


Fig. 1. Comparison of the relative spectral power distributions of three CIE daylight illuminants: (D55) sunlight, (D65) overcast sky, and (D75) north sky daylight along with normalized photopic (V-Lambda) and circadian (C-Lambda) spectral efficiency curves. Note: Both response curves are scaled to have equal area under the curves.

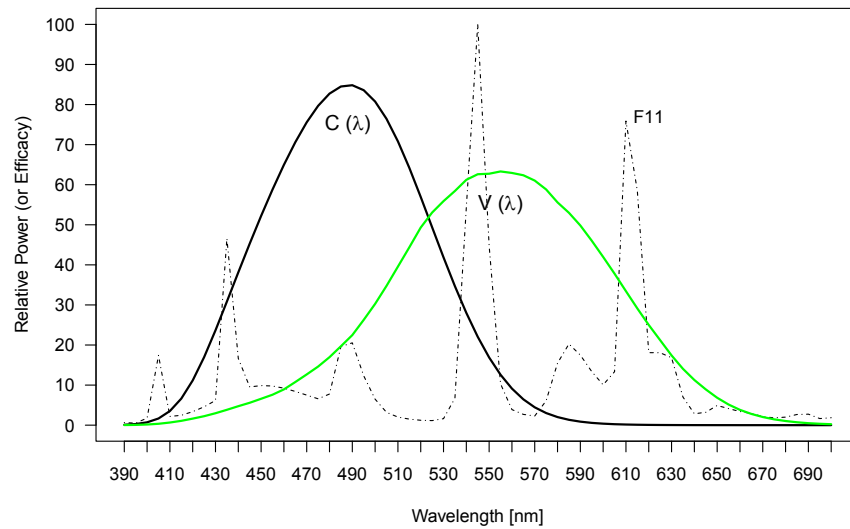


Fig. 2. Comparison of spectral response of the visual system (V-lambda) and the circadian system (C-lambda) to the spectral power distribution of the CIE illuminant F11. Note: Both response curves are scaled to have equal area under the curves.

important consideration, as the relative level of light reaching the retina decreases due to age. Given that buildings should be expected to effectively accommodate a range of ages, the author compared threshold criteria discussed in the following section against a 65-year-old observer model.

A comparison of the EML for various light sources and photopic illuminance levels, along with the resulting biological effect

(melatonin suppression level) is provided in Table 1, which are derived using a 65-year-old observer model. The illuminants “A”, “F11” and “D65” are standard CIE illuminants. Outcomes for a 9500° Kelvin color temperature LED are provided in the final column. For reference, the 65-year-old observer model requires a 6% greater stimulus intensity relative to a 32-year-old to achieve an equivalent effect, or a 11% greater intensity relative to a 10-year-old observer.

Table 1
Biological impact of various light sources and photopic illuminances.

Melatonin suppression (%)	EML	A (Lux)	F 11 (Lux)	D 65 (Lux)	LED 95 (Lux)
0.5	17	29	27	16	14
5.0	34	56	52	31	27
25.0	56	95	87	52	45
50.0	77	129	118	71	62
75.0	105	176	161	97	84
95.0	176	296	272	162	142
99.5	341	575	526	315	275

At present, there is no consensus for the appropriate minimum light exposure threshold to ensure effective circadian stimulus in buildings, or for the duration at which the effects of light exposure saturate. The WELL Building Standard's *Circadian Lighting Design* precondition (option 1) implements a minimum threshold of 250 EML (equivalent to 226 lux from D65), which must be available for at least 4 h each day and can be provided at any point during the day. As noted previously, this requirement can be met with daylight, electrical light (exclusively), or a combination of both sources. The 250 EML threshold and 4-h exposure requirement currently implemented in the WELL Building Standard are based on best judgments derived from recent studies [25,26] and should be expected to be refined as the relationships between spectral distribution, duration, timing, and intensity of light exposure for optimal circadian health are further clarified by the research community. For comparison, Figueiro et al. recommend exposure to a CS of 0.3 or greater at the eye for at least 1 h in the early part of the day (equivalent to 180 lux, D65) [27].

2.1.1. Definition of circadian effect thresholds

While it is arguably too early to propose a precise minimum threshold for adoption in an international standard, it is possible to establish a threshold derived from available research and emerging health-based standards (e.g. WELL) that can serve as an indicator of the presence (or lack) of an effective circadian stimulus at a particular measurement location over a specified time period. The approach taken by the author is to use the same 250 EML threshold implemented by the WELL Building Standard, but segment the analysis to the circadian resetting period of the day (6:00–10:00 a.m.). As shown in Fig. 3, the effect of light on melatonin suppression follows a nonlinear dose-response curve. Using the model provided by Amundadottir et al. [22] (see Fig. 3), which is based on the findings of Cajochen et al. [19] and Zeitzer et al. [25], The 250 EML threshold is shown to predict nearly full saturation (98.5%) in melatonin suppression for a 65-year old observer. For comparison, the light stimuli (in EML) required to achieve 5% and 50% effects are shown as vertical lines in Fig. 3 and listed in Table 1.

2.2. Timing and duration

The timing of light exposure during the day plays an important role in synchronizing the rhythm of the circadian system with daily

rest/activity patterns [28]. Humans possess an internal biological clock that regulates daily patterns of activity following the natural 24-h light/dark cycle. The suprachiasmatic nuclei (SCN) hosts the circadian clock (or circadian system) responsible for orchestrating the daily timing of physical, mental and behavioral changes, for example, sleep/wake, alertness level, mood, hormone suppression/secretion, and core body temperature. The internal period of the human circadian rhythm can range between 23.5 and 24.7 h, with an average of 24.2 h among healthy adults [29] and relies on a resetting response driven by light received at the retina to maintain entrainment with the local 24-h light/dark cycle. Lack of an effective light stimulus at the appropriate time during the day can disrupt the circadian system. For example, most individuals who exhibit total blindness and consequently lack access to a daily resetting response from light suffer from “non 24-h sleep wake disorder,” in which the internal circadian rhythm becomes out of phase with the local 24-h light/dark cycle [30,31]. Disruption of the circadian clock can lead to poor sleep, reduced alertness, and increased risk of a range of health maladies including diabetes, obesity, cardiovascular disease and cancer [32]. As noted by Zelinski et al. [32] the most severe health risks, such as cancer, diabetes, and coronary problems are identified from studies of populations engaged in shift work or employment on a rotating schedule, where an individual is required to deviate his/her sleep/wake pattern from the local 24-h light/dark cycle. For these populations, health risks cannot be addressed by improved access to an effective circadian stimulus during the regular (i.e. 6:00–10:00 a.m.) circadian resetting period. However, these findings illustrate the risk of circadian disruption in humans. Therefore, although the long-term health risks of insufficient or inappropriately-timed light exposure on healthy building occupants working on regular schedules is less established, a precautionary approach warrants the provision of a circadian-effective and appropriately timed light stimulus on a daily basis throughout the year to avoid the risk of circadian disruption.

For a typical well-rested and regularly-sleeping individual, a light stimulus in the early morning will advance the circadian clock, causing earlier wake-up time and earlier sleep onset. Light received in the evening will delay the circadian clock, causing later wake-up time and later sleep-onset. Light received in the middle of the biological day will have limited effect on circadian advancement or delay, but has been shown to cause reduced levels of sleepiness and

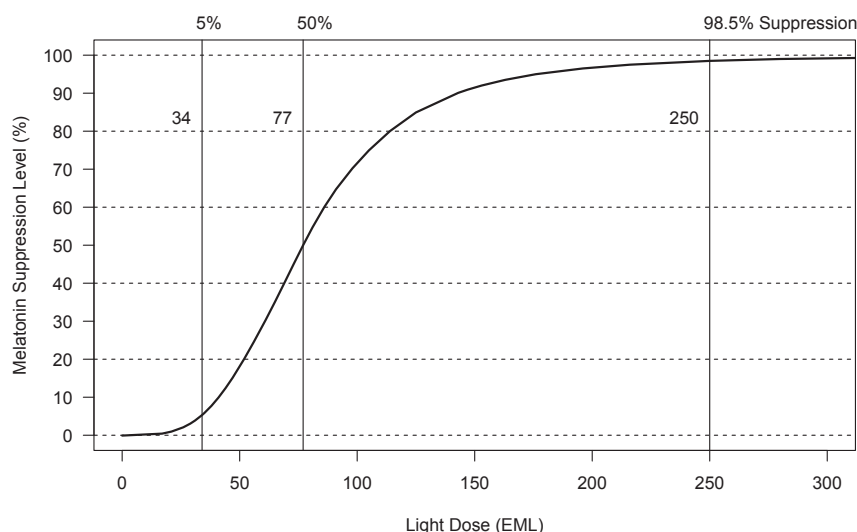


Fig. 3. Dose response curve showing relationship between light exposure and melatonin suppression level.

higher levels of subjective alertness [20,33]. Table 2 provides a summary of the three daily time periods proposed by Ref. [18] to categorize time-varied light exposures according to their expected non-visual effect. Notably, the WELL Building Standard does not specify the time during the day when the light stimulus must be present. Therefore, a space that achieves the compliance criteria (250 EML for 4 h each day) from 12:00–4:00 p.m. could meet the requirement while potentially failing to provide adequate stimulus for circadian resetting during the morning. Finally, past history of light exposure has an effect on sensitivity of the circadian system to light [34]. Higher levels of light exposure during the day cause the sensitivity of the circadian system to decrease over time, and lower exposure levels causes sensitivity to increase. A detailed review of the parameters that control the response of the circadian system to light can be found in Amundadottir et al. [35].

Finally, the regularity of exposure to an effective light stimulus is an important consideration. It is known that sleep and other daily rhythms in physiology and behavior evolved in the natural light/dark cycle. And, it is known that circadian rhythms reflect the programming of biological activities to the periodic nature of the natural environment [36]. Because the natural light/dark cycle follows a recurring (24-h) pattern, it can be argued that the design objective should be to provide an effective circadian stimulus on a daily basis throughout the year. However, circadian rhythms are endogenous in nature, meaning that they are self-sustaining and can persist for a significant period of time in the absence of an external timing cue. And, circadian rhythms take time to adjust when the period of the external timing cue is changed. The observation of an air-traveler's circadian rhythms remaining synchronized with the traveler's original time zone is an example. Therefore, it may be possible to maintain circadian entrainment in buildings even when a stimulus is not present for an individual day, or perhaps multiple days, so long as the stimulus is periodically available within a window of days (e.g. on a weekly or monthly basis). While humans exhibit the ability to adapt and adjust to changes in environmental conditions, it can be argued that a metric addressing the effectiveness of daylight for circadian stimulus should be capable of assessing the regularity of light exposure over a period of time, and capable of differentiating measurement locations where a stimulus is available frequently (e.g. 5 days per week) from infrequently (e.g. 2 days per week). Addressing this task requires the development of methods to assess stimulus frequency for particular view vectors. While the minimum frequency needed to maintain healthy circadian stimulus is not known (e.g. is a stimulus on only Monday, Wednesday, and Friday sufficient?), it can be argued that measurement locations that have more frequent availability of an effective stimulus should be valued over those where availability is less frequent. A preliminary approach to measuring stimulus frequency is presented in Section 3.5 and integrated into the circadian daylight metric proposed by the author.

2.3. Previous work relating circadian entrainment to architecture

Daylighting guidance has only recently begun to shift from the near universal application of the Daylight Factor (DF) approach

towards climate-and-context-representative Climate Based Daylight Modeling (CBDM) [37,38]. While one of the stated objectives of the current LEED Daylight EQ credit compliance approach is to “reinforce circadian rhythms,” the reliance of the compliance process on the metric Spatial Daylight Autonomy (sDA) [39] is problematic as a proxy indicator for non-visual effects of daylight for several reasons. First, the procedures to calculate sDA are not sensitive to timing of light during the day. For example, morning light exposure will have an advancing effect on the circadian clock, while early evening exposure will have a delaying effect. sDA is calculated by taking a count of all analysis grid point locations that achieve the specified Daylight Autonomy (DA) threshold of 300 lux horizontal illuminance for at least 50% of occupied hours during the year (eg. 8:00–18:00, Monday-Friday), and dividing the count by the total number of analysis grid points to determine the spatial average. Thus, a workspace could meet the DA criterion without the presence of any daylight during the morning circadian resetting period (6:00–10:00 a.m.) [18]. Second, the sDA metric relies on horizontal illuminance measurements which are recommended to be acquired on a workplane located 0.72 m (30in) from the floor. However, the circadian system responds to vertical light exposure at eye level. Third, the current illuminance threshold of 300 lux exceeds the level of daylight illuminance needed for circadian stimulus and thus discounts hours that may be effective for circadian stimulus. Fourth, the procedures to calculate sDA allow for substantial temporal periods where daylight illuminances are allowed to fall below the specified thresholds. For example, assuming a project is occupied 2000 h per year, a grid point location could fail to meet a given threshold illuminance for 999 of the 2000 total occupied hours and still be considered Daylight Autonomous. Such an outcome is problematic for the maintenance of the human circadian system due to the need for regular (i.e. daily) exposure to sufficient light. Finally, the LEED compliance procedures reward projects where only a portion of the regularly occupied space must meet the compliance criteria (e.g. 55% or 75% of floor area). Due to the significant health risks of circadian disruption, regularly occupied areas of a project that do not meet minimum performance requirements for circadian stimulus should be clearly delineated to ensure that alternate means of effective circadian stimulus are provided to occupants.

Preliminary steps have been taken to develop calculation methods and workflows utilizing lighting simulation software to investigate the non-visual effects of daylight in buildings. Working in collaboration, Andersen et al. [18] and Mardaljevic et al. [40] have proposed a preliminary framework for predicting the non-visual effects of daylight, informed by a review of outcomes of photobiology research. The framework incorporates a photobiology-based lighting model to predict the magnitude and direction of a circadian effect based on parameters of intensity of vertical illuminance at the eye, light source spectrum, and timing (over a 24-h period). Mardaljevic et al. implemented the model in an “in house” climate-based daylight modeling software workflow. The workflow is sensitive to the spectral character of the estimated sky condition to the degree that it differentiates between three CIE illuminant types (D55, D65 and D75) to account for relative

Table 2
Subdivision of Day Based on Non-visual Effect (After Andersen et al.).

Daily time period	Non-visual effect	Description
6:00–10:00	Circadian resetting	Sufficient daylight illuminance can serve to phase advance the clock in the majority of people.
10:00–18:00	Alerting effects of daylight	High levels of daylight illuminance may lead to increased levels of subjective alertness without exerting substantial phase shifting effects on the clock
18:00–6:00	Bright light avoidance	Daylight exposure that might trigger the non-visual effect is to be avoided so as not to disrupt the natural wake-sleep cycle

differences in their contribution to circadian stimulus. The output of the framework is a graphic, color-coded visualization which presents a cumulative, annual summary of the occurrence of non-visual effects (the “circadian potential”) for a specified set of locations and for four viewing directions per location, each split by periods of the day and reported on a scale ranging from 0% (low likelihood of alerting effect) to 100% (high likelihood).

More recently, Inanici et al. [41] developed a simulation procedure to more accurately compute the spectral content of light for the purpose of analysis using circadian lighting indicators such as EML. The procedure is referred to as multi-spectral lighting simulation and adopts the technique developed by Ruppertsberg and Bloj [42,43] who were focused on improving the color simulation accuracy of the lighting simulation engine Radiance [44]. The procedure is implemented in a free software tool (Grasshopper plugin) entitled “Lark Spectral Lighting” which can be used by designers to analyze luminance renderings and irradiance data to obtain point-in-time calculations of EML [45]. The primary limitation of this tool is that it currently cannot be applied to annual, hourly analyses. It is anticipated that promising tools such as Lark will become integrated into CBDM workflows, enabling more accurate grid-based time-series lighting data. The procedures presented in this paper are essentially a post-process on such lighting data and serve as a metric for annual evaluation that will become more precise as simulation methodologies continue to evolve and improve.

Even with the capability to generate spectrally accurate, spatialized (e.g. grid-based) time-series data over an annual period, there is still the task of appropriately interpreting, summarizing and visualizing performance outcomes to inform the design process. The approach developed by Andersen and Mardaljevic [18,40] has several limitations in this regard that should be considered. The procedure reports a cumulative measure of “circadian potential” for each view direction (separated by time of day) that is calculated by taking the arithmetic mean of all illuminance values recorded annually. Therefore, an outcome of 30% could indicate 100% circadian potential for 30% of the year, or 30% circadian potential for 100% of the year. While the latter outcome would indicate an acceptable location for regular and effective circadian entrainment, the former case would be problematic because the level of light exposure is insufficient for 70% of the year. When exterior daylight is available during the year, designers should work with the goal of providing an effective level of daylight stimulus to regularly occupied areas on a daily basis. Therefore, designers need feedback indicating the periods of the year when a given design option results in sufficient or insufficient daylighting conditions for circadian stimulus. This information is needed to delineate the presence or quantify the relative size of zones (e.g. floor area) that should be considered biologically dark, which designers would seek to minimize during the design process. Second, the procedure developed by Andersen and Mardaljevic to summarize the annual performance of a given project reports the arithmetic mean of all sensor locations and all view directions. Taking the arithmetic mean of grid-based illuminance results (i.e. all points and all views over all analysis hours) is ambiguous in regard to the presence and relative size of zones of biological darkness and can easily mask the presence of biologically dark zones in comparisons between various design alternatives. For example, strategy 1 may produce a space with a zone of high circadian potential (e.g. side-lit perimeter zone) and a zone of biological darkness (e.g. core zone), but could result in the same overall mean score (e.g. 50%) as a space having no biologically dark zones, where in fact these lighting environments are significantly different. Importantly, the former could pose significant potential health risks to occupants in the absence of supplemental electrical lighting capable of circadian stimulus, or

occupant behavioral adjustments (e.g. moving to better daylit zone for a period of time during the morning). Addressing these limitations requires the additional assumption of a minimum acceptability threshold for daylight exposure and consideration of how time-varying annual daylight exposures from multiple views for each location should be summarized. Finally, the “in house” workflow developed by Mardaljevic is not publically available and thus cannot be incorporated into the workflows used by designers to inform decision-making.

3. Method

The following sections describe the procedures developed for quantifying and mapping circadian effectiveness in terms of the frequency of a circadian-effective daylight stimulus. Area-based summaries of each spatial category can then be used as indicators to assess and differentiate the performance of various daylighting strategies during the design phases of a project, or to quantify the circadian effectiveness of existing spaces.

3.1. View-point orientation and spatial considerations

The first step in the procedure is to obtain hourly illuminance measurements for each view direction. A horizontal measurement grid is defined and positioned at a distance from the floor specified by the user to represent either seated or standing eye-height. Fig. 4 presents an example showing the measurement grid (0.5 m spacing) generated for analysis of a portable school classroom where eye-height is assumed to be 1.2 m. At each grid point, multiple vectors are arrayed at even increments to represent all possible view directions. In Fig. 4, eight (8) vectors are specified, however the user can increase this number for greater precision. Each vector is then used to define the orientation of a global vertical illuminance sensor in Radiance.

The room geometry and project orientation are modeled in the 3-D modeling software Rhinoceros [46] and imported into Grasshopper [47], where Radiance materials are assigned to all surfaces using the open-source plugin Honeybee [48]. Relevant information related to the model is presented in Table 3 and Radiance parameters in Table 4. An annual climate-based daylighting simulation is then performed with Radiance and Daysim [49] to obtain hourly illuminance measurements for each view direction.

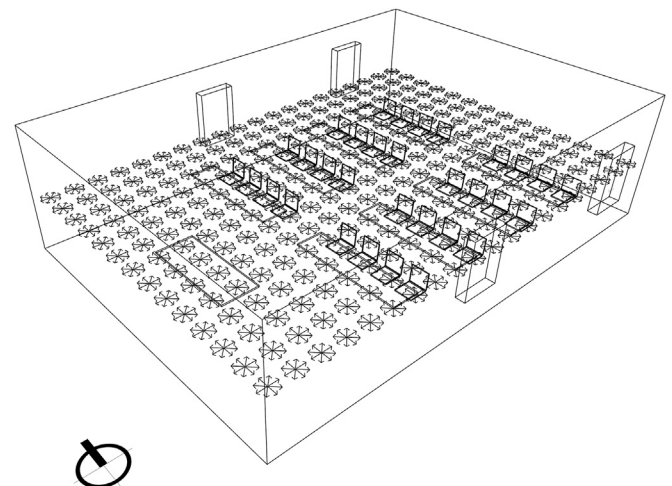


Fig. 4. Perspective view of analysis grid (0.5 m grid-spacing) with eight view vectors per grid point, positioned at a 1.2 m distance from the floor.

Table 3
Model properties.

Property	Value
Window size	0.9 m by 1.5 m
Floor plate length (E-W)	10 m
Floor plate depth (N-S)	7 m
Ceiling height	3 m
Surface reflectance (interior floor)	0.3
Surface reflectance (interior wall)	0.5
Surface reflectance (interior ceiling)	0.8
Glazing visible light transmittance (VLT)	0.65
Climate	San Francisco, CA
Analysis grid spacing	0.5 m
Number of view vectors per grid point	8

Table 4
Model radiance parameters.

Parameters		
av = 0	ps = 4	pj = 0.9
ab = 6	ar = 64	dp = 256
dc = 0.5	as = 2048	dt = 0.25
aa = 0.2	ds = 0.25	lr = 6
ad = 2048	pt = 0.1	dj = 0.5
st = 0.5	dr = 1	lw = 0.01

3.2. Calculation of EML based on the relative direct and diffuse magnitudes

Illuminance measurements (reported in lux) are converted to EML using a conversion factor (ranging from 1.0 to 1.10) to predict the actual source efficacy for each hour based on the relative direct and diffuse illuminance magnitudes reported in the climate data file. Diffuse illuminance is assumed to correspond to D65, which has a “circadian efficacy” of 1.10 (i.e. the conversion factor from photopic lux to EML is 1.10). Direct illuminance is assumed to correspond to D55, which has a circadian efficacy of 1.0. Thus, a direct illuminance of 60,000 lux concurrent with a diffuse illuminance of 15,000 lux leads to a conversion factor of $(0.8 \times 1.0 + 0.2 \times 1.10 = 1.02)$. Fig. 5 shows the hourly variation in the modified conversion factor using climate data from a location in San Francisco, CA. It is important to note that the current approach to determine eye-level EML exposures from illuminance results does not account for the modification of the relative spectrum of light by glass (e.g. spectrally selective glass) or non-neutral internal surfaces (e.g. colorful walls, floors or ceilings).

3.3. Time periods of analysis

In the present workflow, three times of day were defined

following the schema developed by Andersen et al. [18] (Table 2) to assess circadian potential. These are 6:00–10:00 a.m. (*circadian resetting*), 10:00–18:00 (*alerting effects of daylight*), and 18:00–6:00 (*bright light avoidance, dim light only*). Access to bright, circadian effective light in the morning is most critical for circadian resetting. However, it is important to note that exposure to bright light during the 10:00–18:00 period may be desirable (and preferred) by occupants for its potential to increase alertness. In the present example, the analysis focuses on the circadian-resetting period (6:00–10:00 a.m.) annually, and the hour 6:00–7:00 a.m. is removed from analysis on the basis that the space would be unoccupied during this hour.

3.4. Daily spatial assessment of circadian stimulus

Hourly EML results within the time period 7:00–10:00 a.m. are evaluated to determine all vectors that achieve the minimum stimulus requirement (250 EML) for all three analysis hours. Such vectors are then defined as *Circadian-Effective* (CE) for that day. Fig. 6 shows the result for March 19 (predominantly overcast skies) as an example, where red is used to identify each CE view vector. Fig. 7 shows the result during the same time period for the following day (March 20, clear skies). Comparison between Figs. 6 and 7 shows how daily variations in sky conditions can lead to significant changes in the location, orientation, and quantity of CE views. The visualization of daily CE view results can provide valuable feedback to designers on the dynamic nature of circadian effective area in the space. However, it would likely become burdensome to visually examine 365 individual images. The challenge is to understand and quantify daily variations in the availability of an effective stimulus for each measurement location in a space to begin to examine the “quality” of circadian entrainment. This challenge is addressed in the following section.

3.5. Calculation of stimulus frequency

While the availability of a circadian-effective stimulus can be easily determined on a daily basis, additional assumptions are required to assess the effectiveness of the stimulus in maintaining entrainment over period of time, such as a week, month, or year. Examination of data from a single grid-point location from the classroom model illustrates this challenge. Fig. 8 uses a polar plot to display each day of the year (365 analysis days) where the daily circadian stimulus criteria was met (grey) by at least one view from grid point location # 159 (see asterisk in Fig. 7). In this example, compliance for each grid-point is based on a *best vector* approach, which considers a stimulus present for a given day if at least one of the 8 available view vectors meets the daily stimulus criteria (i.e. ≥ 250 EML from 7:00–10:00 a.m.). The *best vector* approach is

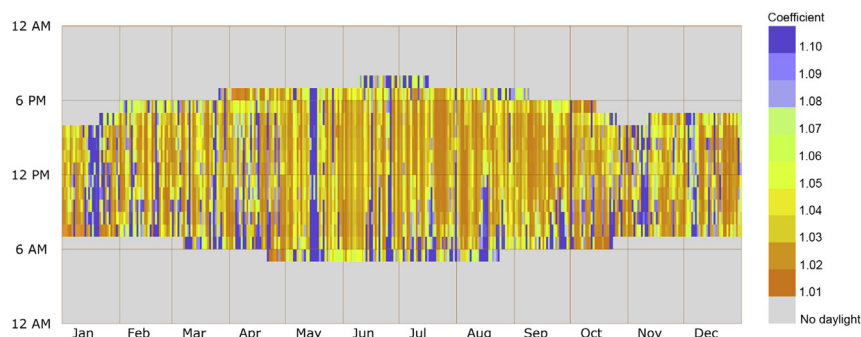


Fig. 5. Annual variation in spectral weighting coefficient derived from San Francisco, CA direct and diffuse illuminance data.

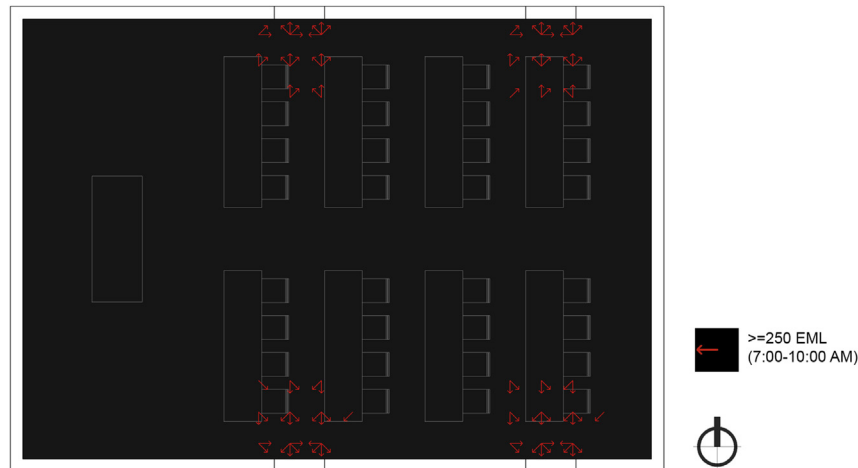


Fig. 6. Plan view of classroom showing views that meet the minimum stimulus criteria (≥ 250 EML from 7:00 to 10:00 a.m.) for March 19 under predominantly overcast sky conditions.

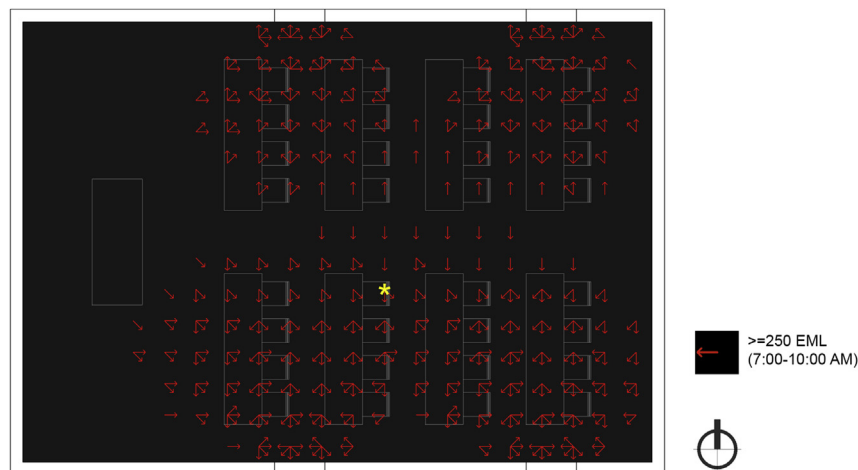


Fig. 7. Plan view of classroom showing views that meet the minimum stimulus criteria (≥ 250 EML from 7:00 to 10:00 a.m.) for March 20 under predominantly clear sky conditions. The yellow asterisk indicates the viewpoint location examined in Section 3.5. (For interpretation of the references to colour in this figure legend, the reader is referred to the web version of this article.)

developed to identify the potential provided by a given daylighting strategy for maintaining healthy circadian entrainment in early stage design, prior to definition of specific (e.g. fixed) views that may be imposed by furnishings or other elements. Even with the *best vector* approach, an effective stimulus is only available for 58% of days during the year (210 of 365 days) for grid-point #159. Because the stimulus is not available during December and January, the location can be easily identified as problematic for that seasonal period. The remaining 10 months are more challenging. During these months, February through November, a CE stimulus is present, but its daily availability is not continuous. For example, there is a regular daily CE stimulus during the first 1.5 weeks of June, but then it becomes more fragmented.

To quantify variations in the availability of a CE stimulus over a period of time (e.g. one week), the author developed the indicator *stimulus frequency* (*stim.freq*). A *stim.freq* score is calculated for each view on a daily basis. The score is calculated as a percentage of the current and trailing X-days, and serves as an indicator of how frequently a daily stimulus was present over the specified window of time (e.g. 1 week). Fig. 9 presents an example of daily exposure scenarios leading to varying *stim.freq* outcomes, based on the

current day (day 7) and trailing 6 days (days 1–6). The 7-day window is a judgment made by the author based on an assumption of the “length” of light history that is necessary to examine in order to make a reasonable assessment of the health impact on the occupant. For example, lack of an effective stimulus over 7 days can be considered problematic for circadian disruption. Similarly, an effective stimulus for only one or two days within the analysis window may also be problematic, but is less of a risk relative to zero days. As the calculated frequency increases, the level of risk decreases. Using a moving analysis window of 7 days, monthly and seasonal *stim.freq* trends can be examined to assess variations in the frequency of an effective stimulus. Times of the year when a daily stimulus is more frequent can then be graded higher than times when stimulus is less frequent, or not present. It should be noted that in the following examples, the analysis is applied to all days of the year for the purpose of simplicity and to account for the fact that commercial buildings may be occupied on weekends. Where the scheduled occupancy of a project is known to not include weekends, these days could be excluded from analysis.

Fig. 9 shows a provisional grouping of *stim.freq* levels into five letter grades (A,B,C,D,F) that represent variations in the *entrainment*

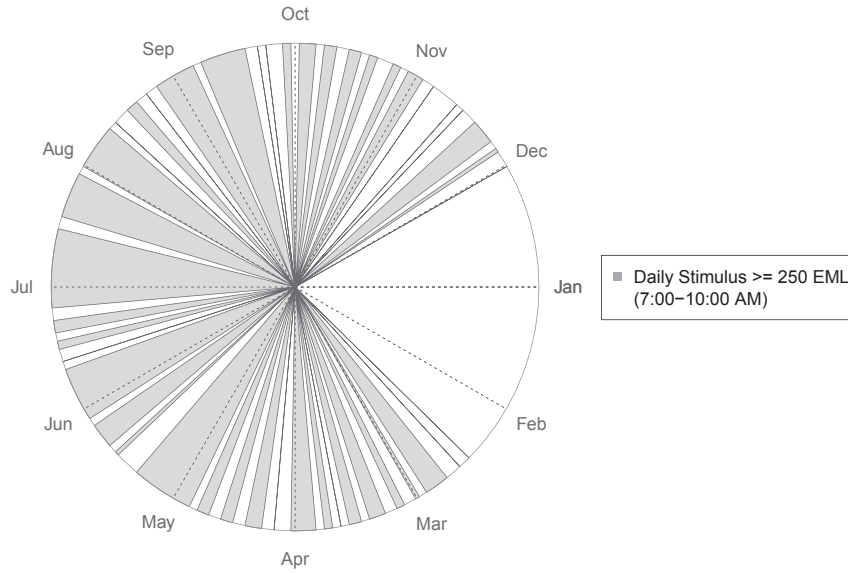


Fig. 8. Daily variation in presence of CE stimulus for a single grid point location (grid point #159) using the *best vector* approach to determine if location meets daily stimulus requirement.

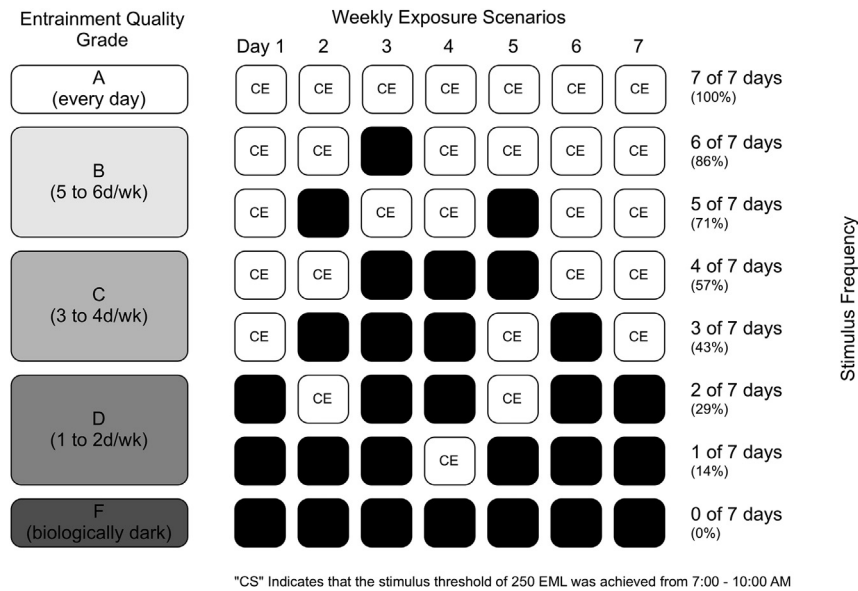


Fig. 9. Hypothetical daily exposure scenarios leading to varying *stimulus frequency* outcomes. Shown on the left are the five grades (A, B, C, D, F) developed to differentiate levels of *entrainment quality*.

quality achieved for a given location. A regularly occurring “A” grade for a grid point location over a period of the year (e.g. the month of June) indicates a location in space that can be easily labeled as *circadian effective*. Alternatively, a grid point that regularly achieves an “F” indicates a location that can easily be labeled as *biologically dark*. The intermediate cases represent variations in performance that are more challenging to label. For example, Fig. 10 presents the resulting *stim.freq* outcomes for grid point #159 based on the frequency of daily exposure shown in Fig. 8 and using a 7-day analysis window. Not surprisingly, the *stim.freq* outcome is often variable. To assess when during the year the *stim.freq* is acceptable and unacceptable for maintaining healthy circadian entrainment, an additional assumption is required for the minimum acceptable *stim.freq* level. In Fig. 10, a threshold of 71% is applied, indicating the requirement of an effective stimulus for at

least 5 days within any 7-day period (equivalent to maintaining an “A” or “B” *entrainment quality* grade, Fig. 9). This assumption is based on the rationale that an effective stimulus should be available on a daily basis, but that one or two days per week where an effective stimulus is not present would present a minimal risk for circadian disruption. Presently, the relationship between exposure to various *stim.freq* levels and risk for circadian disruption is not known. However, it can be argued that a greater *stim.freq* level (e.g. 86%, 6 of 7 days) will always be valued over a lower level (e.g. 29%, 2 of 7 days). Therefore, *stim.freq* can be applied as a provisional indicator of variations in the *entrainment quality* of a daylight space. The following sections present an approach for visualizing and quantifying spatial and temporal variations in *stim.freq*.

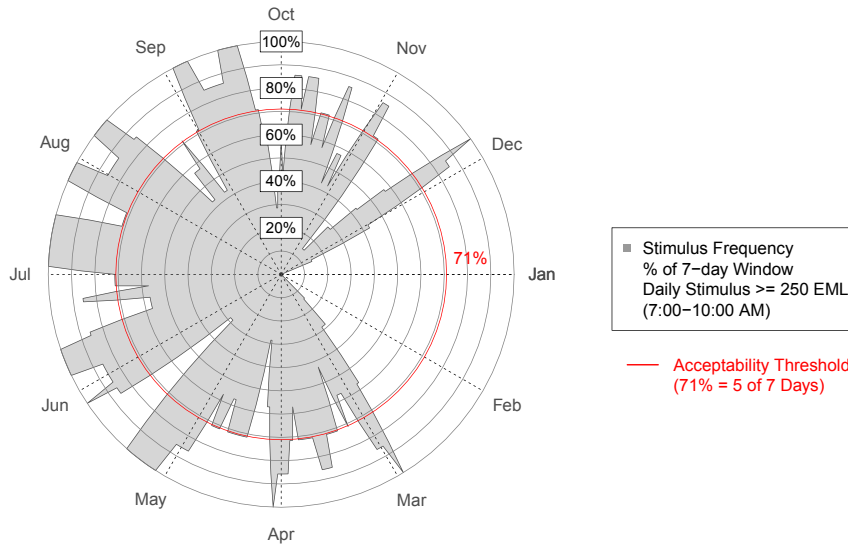


Fig. 10. Stimulus Frequency calculated for grid point #159. Calculation is based on assessment of circadian stimulus level on a daily basis within moving 7-day window (current day and trailing 6 days).

3.6. Calculation of circadian effective area (CEA)

The *Circadian Effective Area (CEA)* of a space is defined as the percentage of analysis area that meets or exceeds the minimum acceptable *stim.freq* threshold on a daily basis. Fig. 11 presents an annual visualization of daily CEA (0–100%) for the classroom model based on varying *stim.freq* threshold requirements ranging from 7-days/week to 1-day/week for a San Francisco climate during the circadian resetting period (7:00–10:00 a.m.) and including all (365) days of the year. Fig. 12 presents results for the same model situated in Helsinki, Finland. The annual mean CEA (0–100%) for both climates are presented in Table 5 for a range of various *stim.freq* threshold possibilities. Comparison between Figs. 11 and 12 shows

that in both climates, the daily CEA is less variable as the threshold is reduced (e.g. from 7d/wk to 4d/wk) and that neither location is capable of achieving 100% CEA at any point during the year, regardless of the minimum *stim.freq* level specified. Polar-plots of daily CEA, such as Figs. 11 and 12 can be used to visually assess daily and seasonal variations in performance and are applicable for comparisons between projects in different climates. The annual mean CEA (Table 5) for a given threshold (e.g. 5d/wk) serves as a summary indicator that can be used to assess the relative performance of various daylighting strategies for a single climate. Table 6 presents annual mean CEA achieved within each *entrainment quality grade* (A,B,C,D,F). When reported by grade (Table 6), the percentages of analysis area that fall within each grade sum to

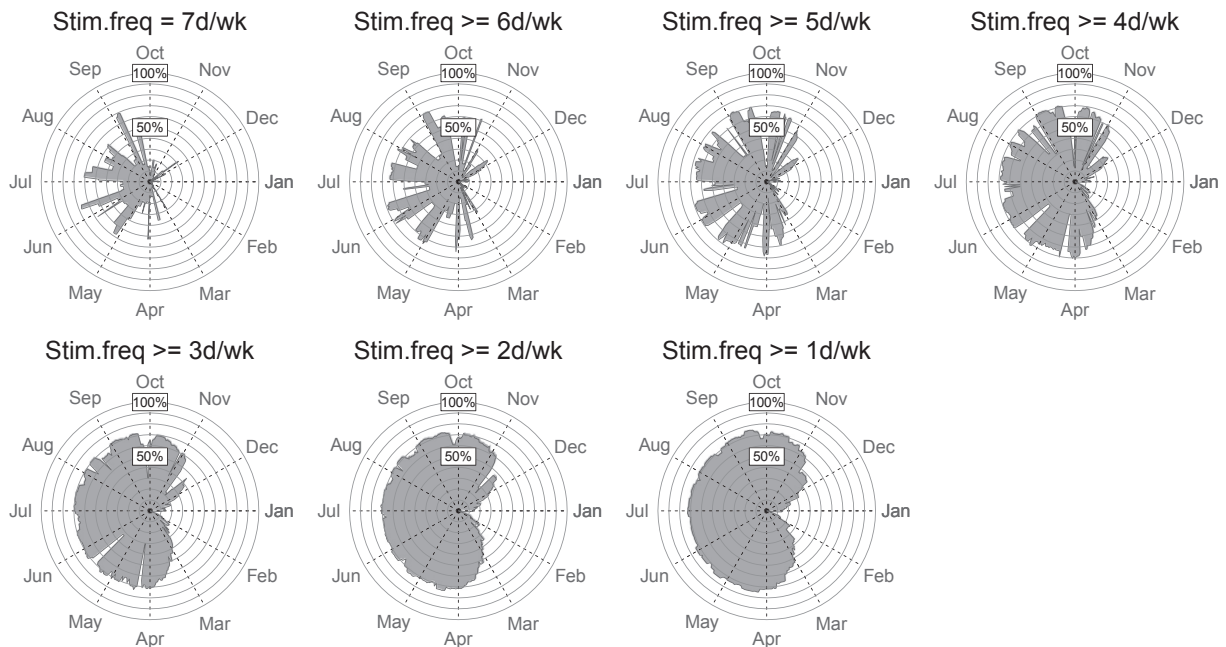


Fig. 11. Annual visualization of daily Circadian Effective Area (0–100%) for classroom model based on varying stimulus frequency threshold requirements ranging from 7-days/week to 1-day/week (San Francisco climate data).

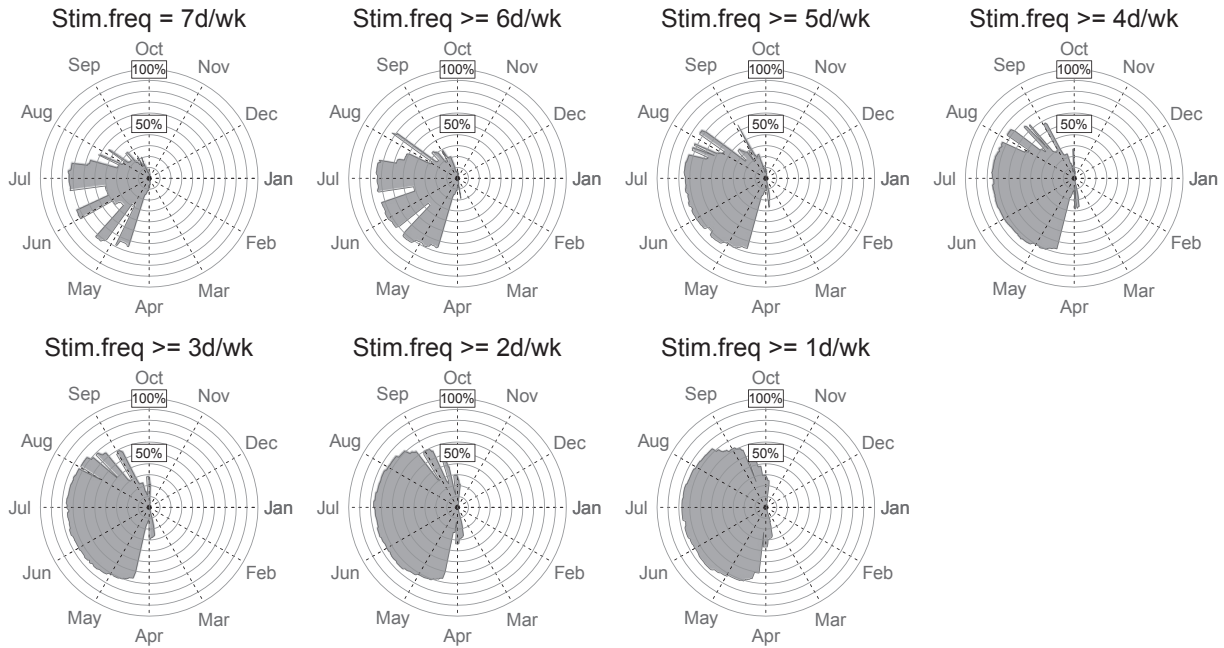


Fig. 12. Annual visualization of daily Circadian Effective Area (0–100%) for classroom model using Helsinki climate data.

Table 5
Annual mean circadian effective area (0–100%) exceeding various stimulus frequency thresholds (7d/wk to 1d/wk).

Climate	Days/week when EML stimulus was achieved						
	7d	≥6d	≥5d	≥4d	≥3d	≥2d	≥1d
San Francisco	20.5	29.9	38.1	45.5	50.4	53.7	56.2
Helsinki	18.9	23.3	26.6	29.1	31.2	33.4	35.7

Table 6
Annual mean circadian effective area (0–100%) achieved for each entrainment quality grade.

Climate	A	B	C	D	F
	7d/wk	5–6d/wk	3–4d/wk	1–2d/wk	0d/wk
San Francisco	20.5	17.6	12.3	5.8	43.8
Helsinki	18.9	7.7	4.6	4.5	64.3

100%. Therefore, the design objective is to increase the amount of analysis area falling within the higher grades (e.g. A and B), which will then reduce the amount falling within the lower grades (e.g. C and below).

3.7. Spatial mapping of seasonal variations in circadian effective area (CEA)

Fig. 13 presents a proposed visualization format that includes a “stacked” version of the *stim.freq* data in Fig. 11, but grouped within each of the five entrainment quality grades defined in Fig. 9. The twelve floor plans arrayed around Fig. 13 present a spatial mapping of the monthly mean CEA for each of the five grades. This format allows designers to visually understand spatial variations in the presence and quality of the daylight stimulus over an annual period, with reasonable representation of seasonal effects. It should be noted that this image is somewhat compressed so that it can fit within a standard journal paper format, and would likely be expanded to a larger size when viewed by the design team.

3.8. Spatial mapping of annual performance

The visualization format shown in Fig. 13 is more complex than the standard practice of generating a single annualized performance summary. Fig. 14 presents an annual visualization of the circadian effectiveness for the classroom model (San Francisco climate) by reporting the percentage of the year (0–100%) where a minimum *stim.freq* of 71% (5 of 7 days) is achieved (or exceeded) during the circadian-resetting period (7:00–10:00 a.m.). In Fig. 14, the *best vector* approach is used to determine the presence of an effective stimulus at each grid-point location. Annual mapping is useful for understanding the percent of the year (0–100%) when the specified minimum *stim.freq* is achieved (or exceeded) for a particular location within the space. The same technique could also be applied to examine other periods of the day, such as the 10:00–18:00 period, where an alerting effect is of interest. The annual summary allows for variations in performance throughout the space to be identified, where locations that fail to achieve the minimum acceptable *stim.freq* threshold for significant portions of the year can be assessed as higher risk for circadian disruption (in the absence of circadian effective supplemental electrical lighting) relative to locations that regularly meet or exceed the threshold. Designers can also use annual mapping to identify the view orientations that present the greatest potential for circadian entrainment to inform the location and orientation of workstation views. However, the annualized format does not preserve information indicating seasonal variations in performance, or the percentage of the year various grid-point locations achieve other (e.g. more strict or more lenient) *stim.freq* thresholds, and should be relied on after the design team has examined spatial and seasonal variations using the format shown in Fig. 13.

3.9. Treatment of spaces where occupant view orientations are fixed

While using the *best vector* approach is suitable for identifying the circadian “potential” of a given grid point location, the approach is unlikely to be appropriate for spaces where occupants have a

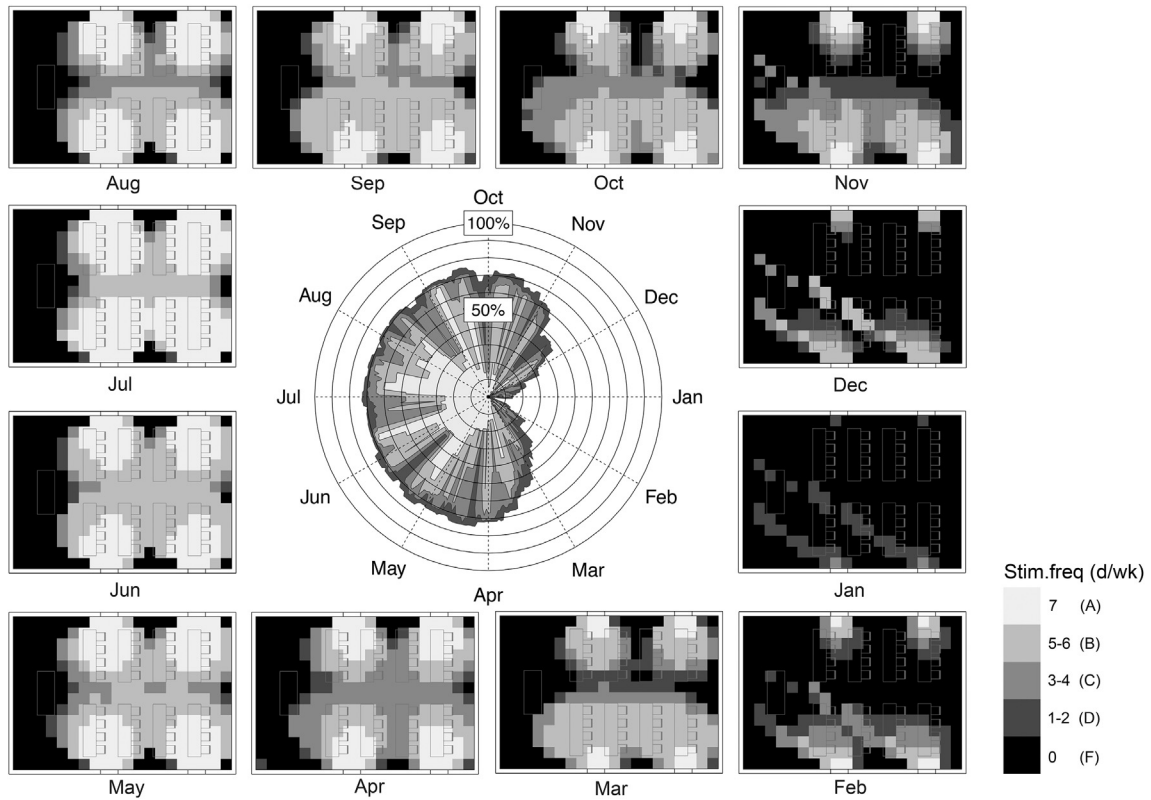


Fig. 13. Combined performance visualization showing daily variation in Circadian Effective Area (CEA) based on varying *entrainment quality grades* (A, B, C, D or F) surrounded by spatial mapping of monthly mean CEA within each of the five grades.

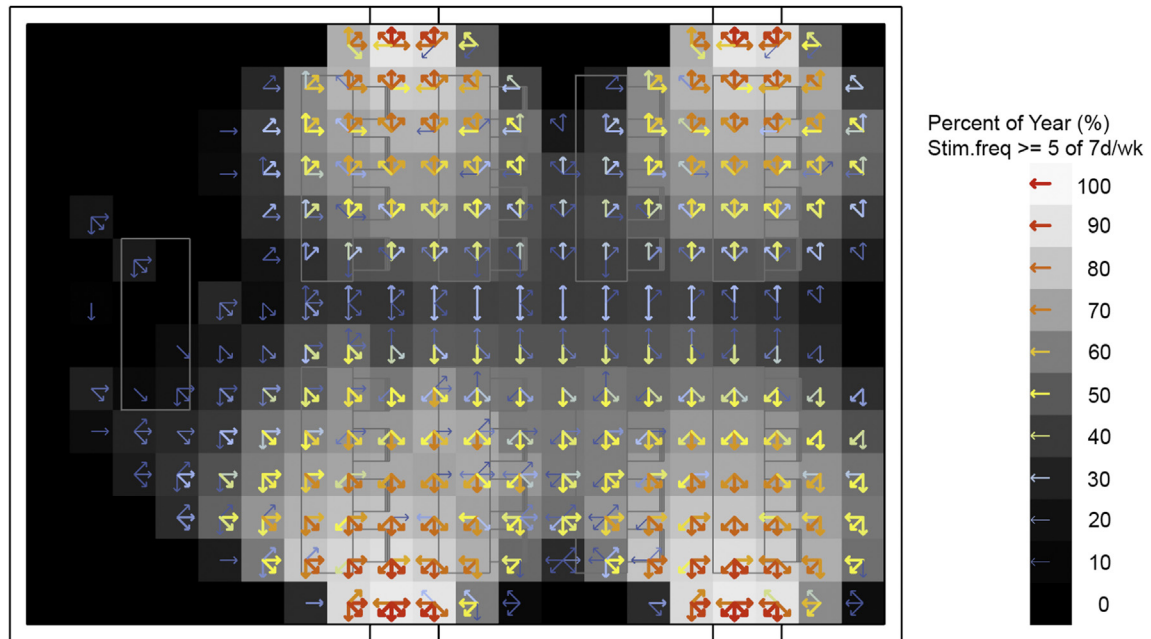


Fig. 14. Annual visualization of the circadian effectiveness of the classroom model (San Francisco climate) showing the percentage of the year (0–100%) where a minimum *stim.freq* threshold of 5d/wk is achieved during the circadian-resetting period (7:00–10:00 a.m.).

relatively fixed viewpoint, such as the present classroom example, where the pre-determined furniture layout indicates a west-facing orientation for those seated at desks. For examination of spaces pre-programmed with largely fixed viewpoints, it may be more

appropriate to constrain analysis to a single view direction, or subset of view directions. Fig. 15 presents an alternate mapping of the classroom using the same vector data from Fig. 14, but restricting analysis to the results of only the west-facing view

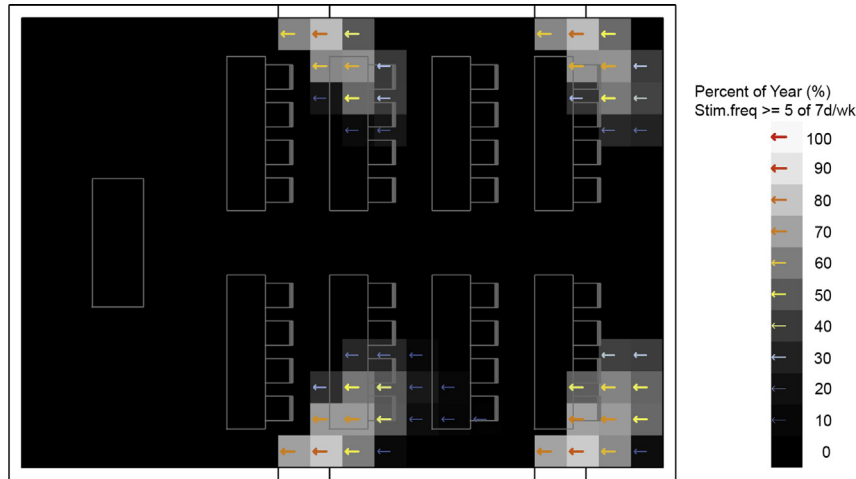


Fig. 15. Alternate spatial mapping of circadian effectiveness based on fixed view direction.

vectors. Comparison between results from the two different approaches (Fig. 14 vs. Fig. 15) illustrates the substantial sensitivity of analysis outcomes to the assumed view orientation(s).

4. Application of spatial classifications to inform design

The following example demonstrates the applicability of the proposed metric for making relative comparisons between design options in early-stage design. For this example, one floor plate from a hypothetical medium-size commercial office building located in San Francisco, CA (Fig. 16) is analyzed to compare the outcomes for two different Window-to-Wall Ratio (WWR) options, 1) a WWR of 0.30 (shown in Fig. 16) and, 2) a WWR of 0.50. The WWR is consistent for all four facades, the Visible Light Transmittance (VLT) of all windows is (0.65), and the models are analyzed without the presence of interior shading devices. Structural columns and an opaque core zone volume are included in the models to represent the level of detail for an early stage of schematic design. The core zone (e.g. elevators, stairs, bathrooms and storage), along with a buffer zone of circulation are excluded from the analysis grid. Relevant model properties are shown in Table 7 (Radiance parameters are identical to the previous example, Table 4). A relatively large analysis grid spacing (2 m) is applied for the purposes of visualization.

Fig. 17 shows the annual result for the 0.30 WWR option for the

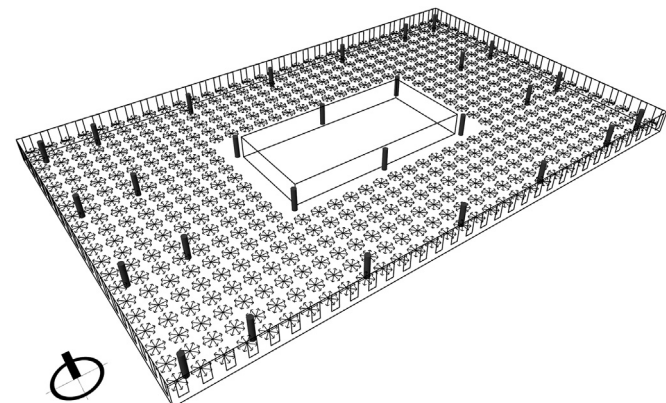


Fig. 16. Perspective view of one floor of medium commercial office building model (0.30 WWR) showing analysis grid and view vectors.

Table 7
Model properties.

Property	Value
Window to wall ratio (WWR)	0.30 (or 0.50)
Floor plate length (E-W)	64 m
Floor plate depth (N-S)	40 m
Ceiling height	3 m
Surface reflectance (interior floor)	0.3
Surface reflectance (interior wall)	0.5
Surface reflectance (interior ceiling)	0.8
Glazing visible light transmittance (VLT)	0.65
Climate	San Francisco, CA
Analysis grid spacing	2 m
Number of view vectors per grid point	8

morning circadian-resetting period (7:00–10:00 a.m.) using the *best vector* approach and a minimum *stim.freq* threshold requirement of 5d/wk (Fig. 9). As a result, the spatial mapping indicates the percentage of the year where each grid-point location achieves at least a “B” *entrainment quality* grade (see Fig. 9). Fig. 18 shows the annual result for the 0.50 WWR option. Comparison between Figs. 17 and 18 allows designers to visualize the spatial implications of a change in WWR from 0.30 to 0.50, for example, the elimination of the small region of analysis area (shown in black in Fig. 17) that never achieves a *stim.freq* ≥ 5 d/wk. Notably, both options show that a significant percentage of the analysis area is circadian effective (achieves a *stim.freq* 5d/wk) for large portions of the year.

Fig. 19 presents a side-by-side comparison between design options (0.30 and 0.50 WWR) where performance can be examined more precisely in terms of daily variations in CEA (0–100%) for each *entrainment quality* grade (A,B,C,D, (F is not plotted)). Fig. 19 shows that the 0.30 WWR option achieves a level of *entrainment quality* above an F grade over nearly 100% of the analysis area for approximately 8 months of the year (March through November). However, the *entrainment quality* is often poor (e.g. C, or D). By comparison, the 0.50 WWR option achieves significant improvements in *entrainment quality* over the 0.30 WWR option, as well as a greater percentage of CEA. For example, Fig. 19 shows that the 0.50 WWR option leads to an “A” grade of *entrainment quality* for nearly 100% of the analysis area over the seasonal period from May through September, and relatively better grades for the remaining period of the year. Notably, both options fail substantially during the month of January, and as more options (e.g. 0.95 WWR) are examined the designer will be able to establish the limits in

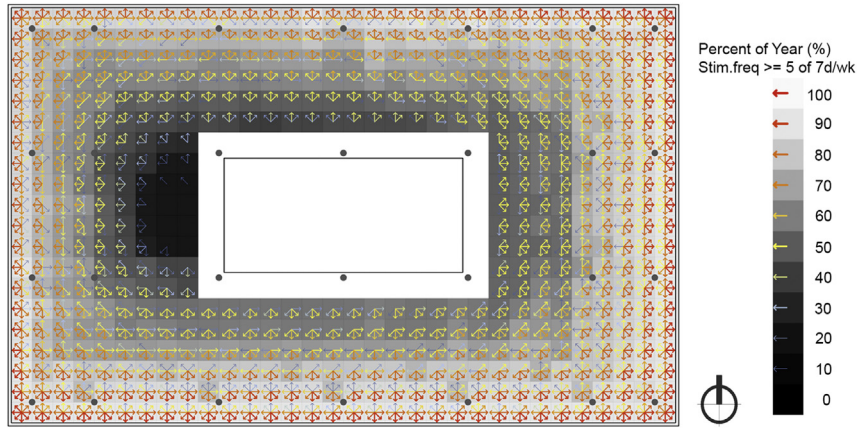


Fig. 17. Plan view of one floor of medium commercial office building model (0.30 WWR) showing annual availability of circadian stimulus ($stim.freq \geq 5d/wk$) based on best vector approach.

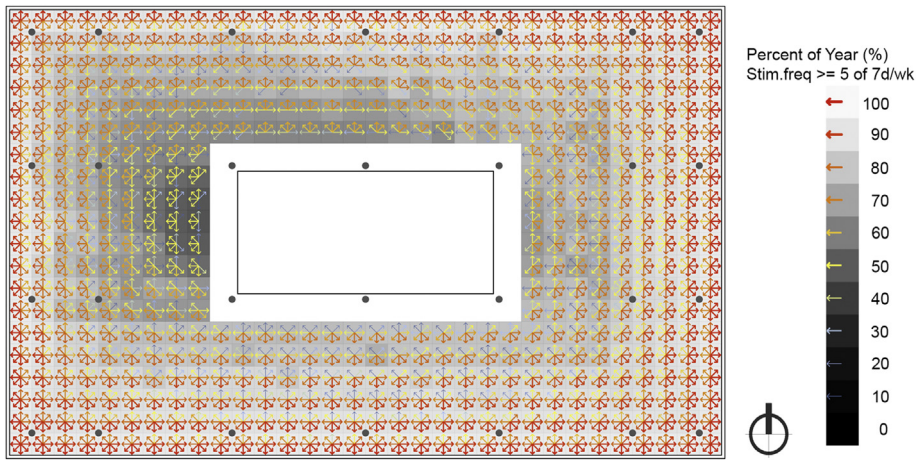


Fig. 18. Plan view of one floor of medium commercial office building model (0.50 WWR) showing annual availability of circadian stimulus ($stim.freq \geq 5d/wk$) based on best vector approach.

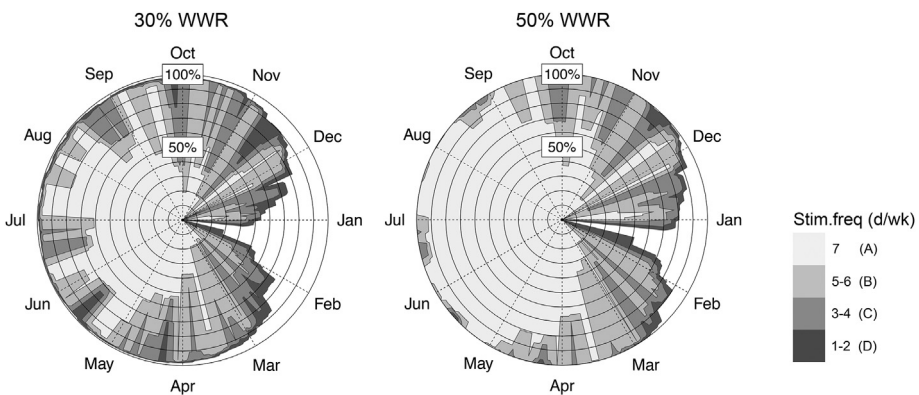


Fig. 19. Comparison of daily variations in Circadian Effective Area (0–100%) between design options (0.30 and 0.50 WWR) for each stimulus frequency grade (A,B,C,D, (F is not plotted)).

performance imposed by latitude and climate. Finally, summarized outcomes reported in terms of mean CEA achieved within each entrainment quality grade (Table 8) can be applied in iterative performance-based design workflows (and in objective functions used by optimization tools) to differentiate the performance of competing design options. For example, a design team would seek

to achieve a solution where 100% of the CEA is achieved with an “A” grade. Given that this optimum may be impossible to reach due to climatic and programmatic constraints, the design team would then favor the option that achieves the greatest percentages of CEA for grades A and B (e.g. the 0.50 WWR option achieves a total CEA for A and B grades of $62.3\% + 21.5\% = 83.8\%$ (Table 8), which is

Table 8
Mean circadian effective area (0–100%) achieved annually for each *entrainment quality grade*.

WWR	A 7d/wk	B 5–6d/wk	C 3–4d/wk	D 1–2d/wk	F 0d/wk
30%	46.0	25.3	12.4	4.6	11.7
50%	62.3	21.5	7.6	2.9	5.7

valued over the 0.30 WWR option of 46% + 25.3% = 71.3%).

4.1. Consideration of fixed viewpoints

The results shown in Section 4 are based on the *best vector* approach, which is developed to identify the potential provided by a given daylighting strategy for maintaining healthy circadian entrainment. In many real projects, programmatic constraints and other design considerations (e.g. glare) may limit the ideal orientation of the occupant view. Figs. 20 and 21 illustrate the impact of various fixed view orientations on performance outcomes for the 0.30 and 0.50 WWR options respectively. Each figure presents annual outcomes for four of the eight specified view orientations and reveals significantly different outcomes relative to the ideal case (e.g. Figs. 17 and 18). For example, the decision to orient workstation views towards the core of the floor-plate would result in “F” grades for a significant number of cases, while views oriented parallel to the facade would achieve the *stim.freq* threshold (≥ 5 d/wk) for a significantly smaller percentage of days during the year relative to views oriented towards the facade. While it is not surprising that the orientation of the view significantly impacts eye-level daylight exposure, it should be noted that current horizontal illuminance measurement practices, such as those applied in LEED Daylight Credit compliance procedures and in various climate-based daylighting metrics do not account for this potential variability. Early in design, analysis of view orientation impacts on circadian daylighting performance can help to inform baseline assumptions for the appropriate orientation of workstation views.

5. Discussion and conclusions

As knowledge of the relationship between lighting parameters and health outcomes increases, new metrics, design frameworks, and field-based evaluation techniques are needed to ensure that all design interventions lead to indoor environments that effectively support the health and well-being of occupants. The area-based circadian daylight metric described in this paper is applicable for informing decision-making in multiple contexts including all phases of the design process, as well as for assessing existing spaces. In early stage design, the goal is to maximize the CEA that achieves the highest *entrainment quality grades* (e.g. A and B) through manipulation of architectural building parameters such as building form, massing, aperture size (e.g. WWR), ceiling height, and other parameters that are set early in the design process. The same goal can be addressed in later stages of design by informing the selection of building components (e.g. glazing and facade shading systems) and controls for lighting and automated shading systems. For the evaluation of existing buildings, the metric can be used to assess and differentiate the performance of multiple spaces that a prospective tenant may choose to occupy, or for a building owner to identify and inform the retrofit of poorly performing zones within a building.

The metric and procedures developed in this paper rely on a number of assumptions for the timing, spectrum, intensity, duration and past history of light exposure needed to maintain effective circadian entrainment. These assumptions are developed from theoretical knowledge, findings from photobiology, and judgments made by the author. Notably, the calculation of *stimulus frequency* (*stim.freq*) and letter grades proposed for *entrainment quality* require assumptions for both the appropriate length of past light history to examine (e.g. current and trailing 6 days) and for the minimum acceptable number of days within that period when an effective stimulus must be present for the exposure scenario to be considered supportive of health circadian entrainment. In this context, the approach developed to assess the duration of an effective stimulus on a daily basis as well as the frequency an effective stimulus is present over the course of a year can be

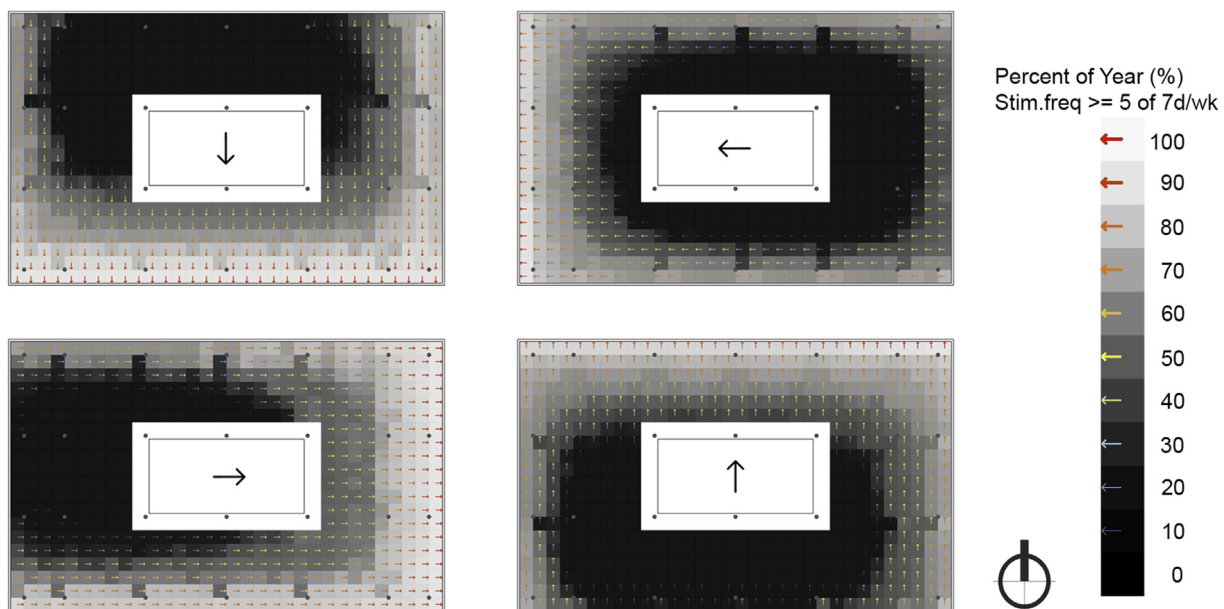


Fig. 20. Plan views of four possible view orientations for the medium commercial office building model (0.30 WWR) showing impact of view orientation (black arrow) on annual availability of circadian stimulus (*stim.freq* ≥ 5 d/wk).

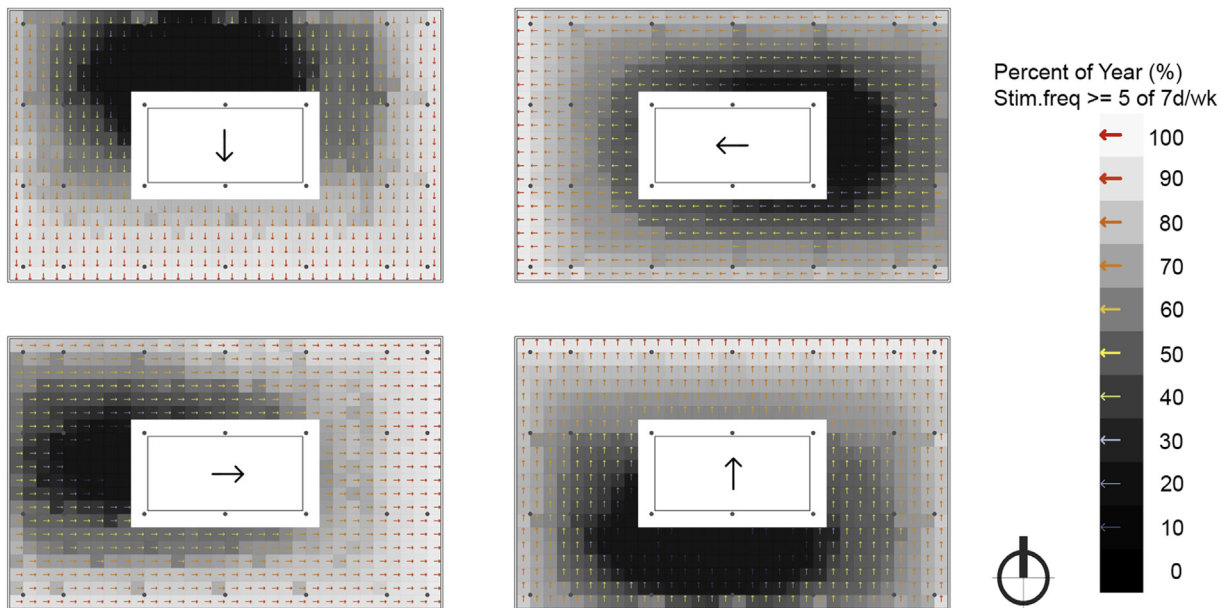


Fig. 21. Plan views of four possible view orientations for the medium commercial office building model (0.50 WWR) showing impact of view orientation (black arrow) on annual availability of circadian stimulus (stim.freq ≥ 5 d/wk).

considered as a preliminary step in addressing the expanded set of assumptions needed to establish health-based lighting metrics. Such assumptions are needed as lighting design shifts from metrics that are based on an assumption of an instantaneous effect (i.e. visual task performance or glare discomfort) to metrics that seek to predict a biological effect that manifests over a length of time and particular pattern of light exposures. The assumptions made in this paper are expected to be refined in response to additional research describing the complex relationship between human biological lighting needs to maintain (or enhance) health and well-being in buildings. The user can adjust the light stimulus thresholds and temporal criteria in the parametric workflow shared with this paper [10] to address specific user populations that may warrant alternate assumptions. For example, it may be determined that a higher minimum daylight illuminance threshold is appropriate for adults older than 65, due to age-related health effects which reduce eye sensitivity to light (e.g. cataracts, glaucoma, macular degeneration). Alternatively, a user can calculate performance results for the *alerting* period of the day (10:00–18:00 *alerting effects of daylight*), in addition to the *circadian resetting* period, or for any arbitrary daily time period.

While theoretical knowledge and scientific findings are sufficient to begin to propose metrics and procedures to classify indoor daylit spaces in terms of anticipated circadian effectiveness, the task of validating the numerous assumptions that underlie such metrics will require a substantial level of field-based validation involving mechanisms capable of collecting feedback from large subject populations in buildings in use [50] in order to compare physical measures of light stimulus with individual health outcomes. It should also be acknowledged that window views can often become a source of glare, which can lead to the deployment of shades, informal occupant modifications to workstations, and in some cases, permanent retrofits to the building facade which reduce daylight transmission [51]. Therefore, efforts to improve the circadian effectiveness of a space should incorporate the use of glare indicators [52] and assessment procedures [53] to understand the relative trade-offs between circadian daylighting and glare.

The transition from metrics based on horizontal workplane

illuminance measurements to new metrics based on vertical, view-based assessments requires new approaches to account for occupant views that may range from dynamic or selectable to fixed. The examples presented in this paper present two basic approaches to identify an appropriate view orientation for analysis. However, more sophisticated approaches can be explored. For example, analysis could be performed on a subset of view vectors for each grid point location, based on an assumption that an occupant has the ability to adjust his/her view within a specified viewing arc (e.g. 45° to the left or right of the primary task view).

The metric and visualization techniques presented in this paper enable designers to specifically address non-visual effects of light during design by making relative comparisons between design alternatives. The metric can also be incorporated into simulation-based workflows incorporating multi-objective optimization, which seek to balance daylighting objectives with whole-building energy use and other performance goals [54]. As a result, the potential health benefits of daylight can begin to be added to the multiple performance objectives used to design and evaluate buildings.

References

- [1] I. Provencio, I.R. Rodriguez, G. Jiang, W.P. Hayes, E.F. Moreira, M.D. Rollag, A novel human opsin in the inner retina, *J. Neurosci.* 20 (2) (2000 Jan 15) 600–605.
- [2] J.J. Gooley, J. Lu, T.C. Chou, T.E. Scammell, C.B. Saper, Melanopsin in cells of origin of the retinohypothalamic tract, *Nat. Neurosci.* 4 (12) (2001 Dec) 1165.
- [3] J. Hannibal 1, P. Hindeross, S.M. Knudsen, B. Georg, J. Fahrenkrug, The photopigment melanopsin is exclusively present in pituitary adenylylate cyclase-activating polypeptide-containing retinal ganglion cells of the retinohypothalamic tract, *J. Neurosci.* 22 (1) (2002 Jan 1). RC191.
- [4] Hattar S1, H.W. Liao, M. Takao, D.M. Berson, K.W. Yau, Melanopsin-containing retinal ganglion cells: architecture, projections, and intrinsic photosensitivity, *Science* 295 (5557) (2002 Feb 8) 1065–1070.
- [5] G.C. Brainard, J.P. Hanifin, J.M. Greeson, B. Byrne, G. Glickman, E. Gerner, M.D. Rollag, Action spectrum for melatonin regulation in humans: evidence for a novel circadian photoreceptor, *J. Neurosci.* 21 (2001) 6405–6412.
- [6] K. Thapan, J. Arendt, D.J. Skene, An action spectrum for melatonin suppression: evidence for a novel non-rod, non-cone photoreceptor system in humans, *J. Physiol.* 535 (2001) 261–267.
- [7] N.E. Klepeis, W.C. Nelson, W.R. Ott, J. Robinson, A.M. Tsang, P. Switzer, J.V. Behar, S. Hern, W. Engelmann, The national human activity pattern survey

- (NHAPS): a resource for assessing exposure to environmental pollutants, *J. Expos. Anal. Environ. Epidemiol.* 11 (3) (2001) 231–252.
- [8] U.S. Green Building Council, LEED v4 for Building Design Construction, April 5, 2016, p. 161. http://www.usgbc.org/sites/default/files/LEED%20v4%20BDC_04_05.16_current.pdf.
- [9] International Well Building Institute. WELL Building Standard (v1), May 2016.
- [10] Zip archive of simulation workflow used in this paper. <https://dl.dropboxusercontent.com/u/4262841/workflow.zip> Accessed 9 August 2016.
- [11] S.W. Lockley, G.C. Brainard, C.A. Czeisler, High sensitivity of the human circadian melatonin rhythm to resetting by short wavelength light, *J. Clin. Endocrinol. Metab.* 88 (9) (2003 Sep) 4502–4505.
- [12] Enezi, et al., A “Melanopic” spectral efficiency function predicts the sensitivity of melanopsin photoreceptors to polychromatic lights, *J. Biol. Rhythms* 26 (2011) 314.
- [13] R.J. Lucas, S.N. Peirson, D.M. Berson, T.M. Brown, H.M. Cooper, et al., Measuring and using light in the melanopsin age, *Trends Neurosci.* 31 (1) (2014) 1–9.
- [14] Lucas et al. Excel-based melanopic illuminance calculator. <http://lucasgroup.labs.manchester.ac.uk/research/measuringmelanopicilluminance/Accessed 25 July 2016>.
- [15] Commission Internationale de l'Éclairage (CIE). <http://cie.co.at/Accessed 19 October 2016>.
- [16] Rea, et al., Modeling the spectral sensitivity of the human circadian system, *Light. Res. Technol.* 44 (4) (December 2012) 386–396.
- [17] Lighting Research Center. Circadian stimulus calculator. <http://www.lrc.rpi.edu/programs/lightHealth/Accessed 8 June 2016>.
- [18] M. Andersen, J. Mardaljevic, S.W. Lockley, A framework for predicting the non-visual effects of daylight - Part I: photobiology-based model, *Light. Res. Technol.* 2012 (44) (2012) 37.
- [19] C. Cajochen, J. Zeitzer, C. Czeisler, D. Dijk, Dose-response relationship for light intensity and ocular and electroencephalographic correlates of human alertness, *Behav. Brain Res.* 115 (2000) 75–83.
- [20] J. Phipps-Nelson, J. Redman, D. Dijk, S. Rajaratnam, Daytime exposure to bright light, as compared to dim light, decreases sleepiness and improves psychomotor vigilance performance, *Sleep* 26 (6) (2003) 695–700.
- [21] C.S. Pechacek, M. Andersen, S.W. Lockley, Preliminary method for prospective analysis of the circadian efficacy of (day) light with applications to healthcare architecture, *Leukos* 5 (2008) 1–26.
- [22] M.L. Amundadottir, S.W. Lockley, M. Andersen, Unified framework to evaluate non-visual spectral effectiveness of light for human health, *Light. Res. Technol.* 0 (2016) 1–24.
- [23] École Polytechnique Fédérale de Lausanne, Interdisciplinary Laboratory of Performance-Integrated Design. SpeKtro, Interactive dashboard for exploring non-visual spectrum lighting. <http://spektro.epfl.ch/Accessed 24 July 2016>.
- [24] J. van de Kraats, D. van Norren, “Optical density of the aging human ocular media in the visible and the UV, *J. Opt. Soc. Am. A* 24 (7) (2007) 1842.
- [25] J.M. Zeitzer, D.J. Dijk, R.E. Kronauer, E.N. Brown, C.A. Czeisler, “Sensitivity of the human circadian pacemaker to nocturnal light: melatonin phase resetting and suppression, *J. Physiol.* 526 (3) (2000) 695–702, <http://dx.doi.org/10.1111/j.1469-7793.2000.00695.x>.
- [26] Chang, et al., Human responses to bright light of different durations, *J. Physiol.* 590 (Pt 13) (2012) 3103–3112, 2012 Jul 1.
- [27] Figueiro, et al., Designing with Circadian Stimulus. *Lighting Design and Applications (LD+A)*, 2016. The magazine of the Illuminating Engineering Society of North America (IESNA). Published October 2016.
- [28] S.B.S. Khalsa, M.E. Jewett, C. Cajochen, C.A. Czeisler, A phase response curve to single bright light pulses in human subjects, *J. Physiol.* 15 (2003) 945–952.
- [29] C.A. Czeisler, J.F. Duffy, T.L. Shanahan, E.N. Brown, J.F. Mitchell, D.W. Rimmer, et al., Stability, precision, and near 24-Hour period of the human circadian pacemaker, *Science* 284 (5423) (1999) 2177–2181.
- [30] S.W. Lockley, D.J. Skene, H. Tabandeh, A.C. Bird, R. Defrance, Relationship between melatonin rhythms and visual loss in the blind, *J. Clin. Endocrinol. Metab.* 82 (11) (1997) 3763–3770.
- [31] S.W. Lockley, D.J. Skene, L.I. Butler, J. Arendt, Sleep and activity rhythms are related to circadian phase in the blind, *Sleep* 22 (5) (1999) 616–623.
- [32] Erin L. Zelinski, Scott H. Deibel, Robert J. McDonald, The trouble with circadian clock dysfunction: multiple deleterious effects on the brain and body, *Neurosci. Biobehav. Rev.* 40 (March 2014) 80–101. <http://www.ncbi.nlm.nih.gov/pubmed/24468109>.
- [33] M. Ruuger, M.C.M. Gordijn, D.G.M. Beersma, B. de Vries, S. Daan, Time-of-day-dependent effects of bright light exposure on human psychophysiology: comparison of daytime and nighttime exposure, *Am. J. Physiol. Reg. I* 290 (5) (2006).
- [34] A.M. Chang, F.A. Scheer, C.A. Czeisler, The human circadian system adapts to prior photic history, *J. Physiol.* 589 (5) (2011) 1095–1102.
- [35] Amundadottir et al. Modeling non-visual responses to light: unifying spectral sensitivity and temporal characteristics in a single model structure. In Proc. of CIE Centenary Conference “Towards a New Century of Light”, Apr 15–16, 2013, Paris, France, p. 101–110.
- [36] C.S. Pittendrigh, Temporal organization: reflections of a Darwinian clock-watcher, *Annu. Rev. Physiol.* 55 (1993) 16–54.
- [37] Mardaljevic J. CIBSE National Conference 2006: Engineering the Future. 21–22 March 2006, Oval Cricket Ground, London, UK.
- [38] J. Mardaljevic, L. Heschong, E.S. Lee, Daylight metrics and energy savings, *Light. Res. Technol.* 0 (2009) 1–23.
- [39] Illuminating Engineering Society (IES), Approved Method: IES Spatial Daylight Autonomy (SDA) and Annual Sunlight Exposure (ASE), 2013, p. 14. ISBN: 978-0-87995-272-3.
- [40] J. Mardaljevic, M. Andersen, N. Roy, J. Christoffersen, A framework for predicting the non-visual effects of daylight - Part II: the simulation model, *Light. Res. Technol.* 2013 (0) (2013) 1–19.
- [41] Inanici M, Brennan M, and Clark E. “Multi-spectral Lighting Simulations: Computing Circadian Light,” International Building Performance Simulation Association (IBPSA) 2015 Conference, Hyderabad, India, December 7-9, 2015.
- [42] A.I. Ruppertsberg, M. Bloj, “Rendering complex scenes for psychophysics using radiance: how accurate can you get? *J. Opt. Soc. A.* 23 (4) (2006) 759–768.
- [43] A.I. Ruppertsberg, M. Bloj, Creating physically accurate visual stimuli for free: spectral rendering with radiance, *Behav. Res. Methods* 40 (1) (2008) 304–308.
- [44] G. Ward, The radiance lighting simulation and rendering system, in: Proceedings of SIGGRAPH 94. Computer Graphics Proceedings, Annual Conference Series, 1994, pp. 459–572.
- [45] Lark Spectral Lighting. http://faculty.washington.edu/inanici/Lark/Lark_home_page.html, Accessed 25 July 2016.
- [46] Rhinoceros 3-D Modeling Program. Robert McNeel & Associates. <http://www.en.na.mcneel.com/contact.htm>, Accessed 19 October 2016.
- [47] Grasshopper Algorithmic Modeling Program for Rhino. <http://www.grasshopper3d.com/>, Accessed 19 October 2016.
- [48] Sadeghipour Roudsari Mostapha, Michelle Pak, Ladybug: a parametric environmental plugin for grasshopper to help designers create an environmentally-conscious design, in: Proceedings of the 13th International IBPSA Conference Held in Lyon, France Aug 25–30th, 2013.
- [49] Daysim, Advanced Daylight Simulation Software, Accessed 19 October 2016, <http://daysim.ning.com/>.
- [50] Konis, K. Leveraging ubiquitous computing as a platform for collecting real-time occupant feedback in buildings. *Intell. Build. Int.* 5(3), 150–161.
- [51] Konis, K. Evaluating daylighting effectiveness and occupant visual comfort in a side-lit open-plan office building in San Francisco, California. *Build. Environ.* 59, 662–677.
- [52] J. Wienold, J. Christoffersen, Evaluation methods and development of a new glare prediction model for daylight environments with the use of CCD cameras, *Energy Build.* 38 (7) (2006) 743–757.
- [53] J.A. Jakubiec, C.F. Reinhart, The ‘adaptive zone’ – a concept for assessing discomfort glare throughout daylight spaces, *Light. Res. Technol.* 44 (2012) 149–170.
- [54] K. Konis, A. Gamas, K. Kensek, Passive performance and building form: an optimization framework for early-stage design support, *Solar Energy* 125 (February 2016) 161–179.